water

Article

Evaluation of Groundwater Infiltration in Sewer Networks Using Fluorescence Spectroscopy

Likai Li [1], Yiwei Li [2], Ping Song [1], Bingjie Fang [2], Haibo Xia [1], Yeyuan Xiao [2,*], Lu Ma [2], Yue Guo [2], Zhongrui Bai [2] and Jiawen Wang [2]

1 Guangdong Guangye Environmental Protection Industry Group Co., Ltd., Guangzhou 510030, China
2 College of Engineering, Shantou University, Shantou 515063, China
* Correspondence: yeyuanxiao@stu.edu.cn

Abstract: Diagnosing water infiltration is imperative to assess the integrity and operation performance of sewer networks, which is challenging and costly due to the complex nature of these networks. This study proposes a simple approach to evaluate the extent of groundwater infiltration via a fluorescence spectroscopy method, i.e., the identification and quantification of the fluorescent signature components of the dissolved organic matter sewage. A newly built sewer network in Shantou, Southern China, was selected for the case study, and a mass balance method based on water quality characteristic factors (total phosphorus and NH_4^+-N) was applied in parallel for comparison. The results showed that the mass balance method was substantially influenced by fluctuations in sewage and external water concentrations, rendering it unreliable due to the extensive data and calculations required. Conversely, three-dimensional excitation–emission matrix–parallel factor analysis enabled the identification of terrestrial humus compounds as the signatures of underground water sources. The estimation indicates that the groundwater proportion across the four surveyed inspection wells along the pipeline network ranged from 10.8 ± 2.5% to 9.6 ± 3.5%, conforming to the allowable groundwater infiltration limits set for municipal sewage pipelines (10–15%). This study presents a simple method for the in-depth analysis of groundwater infiltration in urban sewage networks, providing valuable insights into maintaining water quality and network integrity.

Keywords: three-dimensional excitation–emission matrix–parallel factor analysis; groundwater infiltration; urban sewer network; fluorescent signature components; dissolved organic matter

check for updates

Citation: Li, L.; Li, Y.; Song, P.; Fang, B.; Xia, H.; Xiao, Y.; Ma, L.; Guo, Y.; Bai, Z.; Wang, J. Evaluation of Groundwater Infiltration in Sewer Networks Using Fluorescence Spectroscopy. *Water* **2023**, *15*, 3339. https://doi.org/10.3390/w15193339

Academic Editor: Tianyin Huang

Received: 17 August 2023
Revised: 5 September 2023
Accepted: 12 September 2023
Published: 23 September 2023

1. Introduction

Domestic sewage encompasses water generated from daily human activities. Sewage arising from human excreta is classified as black water, while wastewater from bathing, laundry, and kitchen activities falls under the category of gray water [1]. The ample water resources and high temperatures prevalent in Southern China contribute to significant daily water consumption, particularly for washing purposes [2]. Wang et al. [3] estimated that washing water consumption in Fujian, a sub-tropical province in Southern China, accounted for more than 45% of total domestic water use, while tap water, well water, lake water, and collected rainwater have all been exploited for washing. Within China, centralized sewage systems collect both gray and black water. Notably, the water quality at the same sewage discharge point can vary significantly across different time periods within a single day due to the varying proportions of gray and black water [4]. The sewage is transported through a sewer network, where pollutants undergo degradation [5], and the network may experience the infiltration of low-concentration external water, such as rainwater, groundwater, or surface water. Consequently, while wastewater treatment plants (WWTPs) receive substantial influent volumes, the pollutant concentrations—especially organic matter concentrations in Southern China—remain relatively low [6]. For example, the chemical oxygen demand (COD) concentration in influents to WWTPs in Guangdong

Province is approximately in the range of 80~150 mg/L, which is less than half of the typical value in developed countries [7].

Due to the low organic strength in influents, the WWTPs in Southern China are usually operated far below the design loads, resulting in a significantly reduced cost-effectiveness [8]. The low organic strength also leads to a low ratio of COD to total nitrogen (TN); therefore, the supplementation of external carbon sources, such as acetate or methanol, is widely conducted in these WWTPs to achieve the required biological nutrient removal [7]. This further increases the operating costs of a WWTP. To overcome the problem, it is imperative to understand the relative contributions of external infiltration and internal biotransformation to the reduction in sewage strength [9].

Evaluating the operation of sewage networks and diagnosing water infiltration issues is challenging and costly due to the complex nature of these networks [6]. To address this, Lee et al. employed a GIS database to extract attributes of sewage pipe networks (such as pipe depth, age, size, slope, length, material, and road type) and calculate the probability of leakage in each pipe section [10]. Yang et al. developed a balance model using online monitoring data of rainfall flow, total phosphorus, and COD in sewage treatment plants to quantify the dilution ratio of external water and the degradation of organic matter within sewage networks [6]. However, these methods often overlook the influence of groundwater infiltration and neglect the structural integrity of the sewer system itself. Traditional closed-circuit television (CCTV) inspections of sewer interiors to detect leakage have been found to have limitations [11], e.g., reliance on high-definition cameras, the large workload of image acquisition and processing, the requirement of well-trained and experienced technicians, etc. [12,13]. Moreover, this labor-intensive and error-prone identification method makes it difficult to obtain information on fine-grained sewer defects; therefore, it does not meet the increasing requirements of sewer defect detection [14]. Hence, there is a need to establish a straightforward and feasible evaluation approach for assessing external water infiltration in sewage networks.

In recent years, fluorescence spectroscopy has gained traction for analyzing the composition of dissolved organic matter in sewage [15] and natural water bodies [16]. From the excitation–emission matrix (EEM), the independent underlying fluorescent components can be identified and quantified using the parallel factor analysis (PARAFAC) method [17]. The application of EEM-PARAFAC method has enabled the identification of distinct components of dissolved organic matter from samples [18]. Various fluorescent components typically correspond to different sources of organic pollution [19]. By comparing the fluorescence component intensities, it becomes possible to evaluate the proportion of water from different sources within sewage networks. Parameters like the humification index (HIX), β:α ratio, and biological index (BIX) calculated from fluorescence spectrum data further provide insights into the source and biological metabolism of dissolved organic matter [19].

In this study, we proposed a simple method to quantify external infiltration in sewer networks based on the DOM component proportion and source analysis of fluorescence spectra. A newly constructed segment of an urban sewage network is chosen as the study site for the evaluation of this new method via a comparison with the mass balance method based on water quality characteristic factors (TP and NH_4^+-N). Through continuous multi-point and multi-time monitoring, external water intrusion within the urban sewage network is assessed, and the strengths and weaknesses of both evaluation methods are compared and discussed. This study indicates that the proposed fluorescence spectroscopy method could provide reliable quantitative analysis of external infiltration in sewers and is readily implementable in diverse regions.

2. Materials and Methods

2.1. Site Description

This study mainly evaluated groundwater infiltration in sewer networks; therefore, the study site was selected to avoid the influence of rain and surface water as far as possible. The chosen sewer, spanning a total length of 1.6 km and comprising a trunk sewer with 52 manholes, is situated in the Chaoyang District of Shantou, Guangdong Province (Figure 1). This sewer operates solely on gravity flow and encompasses a continuous course. Notably, it lacks a sewage lifting pump station. The water level within the pipe section remains low, accompanied by a swift flow rate. The upstream inlet serves as the primary source of sewage for the entire sewer stretch, collecting wastewater from a densely populated residential region. Within the middle segment of the sewer, three small domestic sewage outfalls are situated. Importantly, the sewer does not receive industrial wastewater of a production nature. Functioning as a distributary pipe, the sewer holds a high elevation and is relatively unaffected by rainfall. The vicinity of the sewer is devoid of natural water bodies, effectively eliminating their influence.

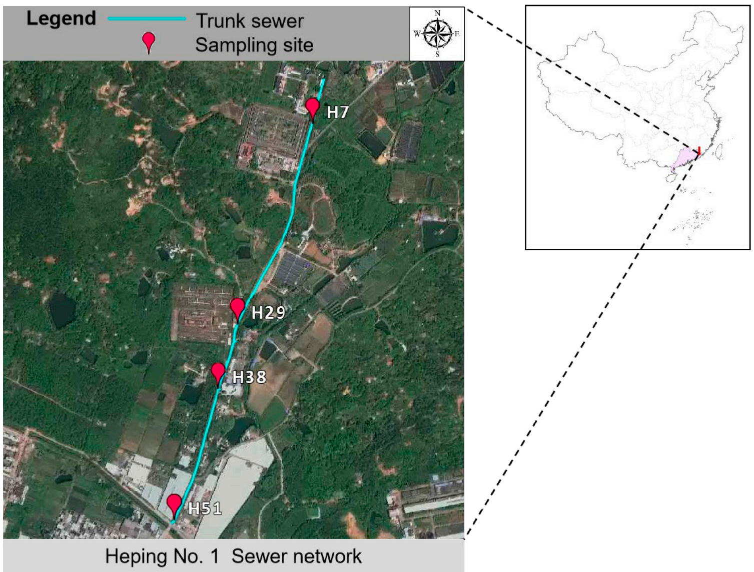

Figure 1. Sampling sites of the sewer networks, Shantou, Guangdong, China.

2.2. Sampling Campaigns and Water Quality Analysis

In this study, four manholes (H7, H29, H38, and H51) were carefully selected along the trunk sewer to represent different points within the sewer network, spanning from its inception to its conclusion. Among these, H7 served as the main sewage inlet, while H29 to H38 encompassed three branch inlets situated in the middle portion of the sewer. These intermediate manholes experienced relatively unstable and small flow rates. To facilitate real-time monitoring of flow fluctuations, flow meters were installed at both the starting point (H7) and the terminating point (H51). The sampling process was conducted continuously at these designated points from upstream to downstream (H7 to H51), occurring every two hours between 8:00 and 22:00 on three distinct dates: 22 March, 23 April, and 26 April 2023. There was no recorded rainfall within the study area for three days before and on the day of sampling.

During the sampling procedure, sewage samples were collected and immediately stored in a cooler at a temperature of 4 °C. These samples were subsequently transported to the laboratory for prompt water quality analysis. The evaluation encompassed the analysis of chemical oxygen demand (COD), total ammonia nitrogen (NH_4^+-N or TAN), and total phosphorus (TP) in the water samples. The determination of biochemical oxygen demand (BOD_5) within the water samples was performed using a BOD_5 determinator from Jiangsu Shengaohua Environmental Protection Technology Co., Ltd. (model: SH-812, Changzhou, China). Furthermore, the concentrations of dissolved organic carbon (DOC) and total dissolved nitrogen (TDN) were measured utilizing a TNM analyzer from Shimadzu (Suzhou, China).

2.3. Fluorescence Spectroscopy Analysis and PARAFAC Modeling

The filtered samples underwent dilution to achieve a total organic carbon (TOC) concentration of 15.0 mg/L. This correction was performed to mitigate the impact of the inner-filter effect. Subsequently, the samples were subjected to analysis using three-dimensional excitation–emission matrix spectroscopy (3D-EEM). The 3D-EEM measurements were conducted utilizing a Hitachi fluorescence spectrophotometer from Tokyo, Japan. The excitation wavelength (Ex) ranged from 220 nm to 500 nm, with a scanning interval of 5 nm, while the emission wavelength (Em) ranged from 250 nm to 500 nm, with a scanning interval of 2 nm. The width of both the Ex and Em slits was maintained at 5 nm. Blank signals from Milli-Q water were subtracted, and fluorescence signals were normalized based on Raman peak areas.

To further assess the obtained EEM data, various indices were calculated. The humification index (HIX), $\beta{:}\alpha$, and biological index (BIX) were derived from the EEM data. HIX represented the ratio of the fluorescence intensity integral value between 435 nm and 480 nm to the fluorescence integral value between 300 nm and 345 nm, both under an excitation wavelength of 254 nm. This index served as an indicator of humus content or the degree of humification [20]. $\beta{:}\alpha$ denoted the ratio of the emission wavelength at 380 nm to the maximum fluorescence intensity within the range of 420 nm to 435 nm, at an excitation wavelength of 310 nm. This ratio reflected the proportion of newly generated colored dissolved organic matter (CDOM) in the overall CDOM and held significance for assessing water biological activity [13]. BIX signified the ratio of fluorescence intensity at an excitation wavelength of 310 nm and an emission wavelength ranging from 380 nm to 430 nm. This ratio provided insights into the relative contribution of autochthonous CDOM within the water samples [14].

The subsequent step encompassed the implementation of parallel factor analysis (PARAFAC) using MATLAB R2016b (MathWorks, Natick, MA, USA), with the aid of the DOMFluor toolbox. The determination of the number of PARAFAC components was based on split-half validation [18]. Each component's fluorescence intensity (Fmax) was employed to represent its concentration level, accounting for TOC concentration. The excitation and emission spectra of each component, as obtained through PARAFAC, were compared against the fluorescence spectra in the OpenFluor database (www.openflour.org, accessed on 20 July 2023). A minimum similarity threshold of 0.95 was considered, and components were deemed similar when this threshold was reached, indicating agreement with components reported in other studies.

2.4. Calculation of Groundwater Infiltration Based on Water Quality Characterization Factors

Due to the relatively short distances between manholes within the study area, the movement of sewage from upstream to downstream manholes occurs rapidly. Hence, it is crucial to identify a water quality parameter that exhibits limited degradability to serve as the equilibrium calculation's water quality characteristic factor. Additionally, this chosen parameter should manifest notably higher concentrations within domestic sewage compared to external water sources, such as groundwater. Given that phosphorus in sewage has a low potential to transform into a gas and escape, its degradation rate within the sewage pipe network remains low. Consequently, total phosphorus (TP) was selected as a suitable water quality characterization factor for this assessment.

Meanwhile, total ammonia nitrogen (TAN) is commonly employed as a water quality characterization parameter for domestic wastewater due to its relevance to sewage [21]. In the current study, both TP and TAN were chosen as water quality characteristic factors, allowing for the computation of groundwater infiltration within the sewage network. This calculation is based on the principle of mass balance, where the input quantity of a substance equals the summation of its accumulation and outflow:

$$\text{Input TP or TAN} = \text{accumulation TP or TAN} + \text{outflow TP or TAN}$$

This mass balance calculation permits the estimation of groundwater intrusion within the sewer network, contributing to a comprehensive understanding of the water quality dynamics within the system.

$$Q_i + Q_j = Q_{i+1} \quad (1)$$

$$Q_iC_i + Q_jC_j = Q_{i+1}C_{i+1} \quad (2)$$

where Q_i represents the flow rate at the upstream manhole and C_i signifies the concentration of the water quality characteristic factor at the same upstream location. Q_j denotes the flow rate of external water infiltration between manholes, and in accordance with the study's context, the dominant source of external water infiltration within this sewer pipeline is groundwater. Q_{i+1} stands for the flow rate at the downstream manhole, and C_{i+1} corresponds to the concentration of the water quality characteristic factor at the downstream manhole.

In consideration of the existence of three branch inlets between manholes H29 and H38, characterized by variable water quality and quantity, it was deemed unsuitable for conducting the study of external water infiltration volume within this segment. Thus, for the assessment of external water intrusion volume, the sections between H7 and H29, as well as H38 and H51, were selected. In accordance with the standards outlined in the Environmental Quality Standard for Surface Water (GB3838-2002), Class III water should exhibit total phosphorus (TP) concentrations not exceeding 0.05 mg/L, while total ammonia nitrogen (TAN) levels should be within or below 1.0 mg/L. Given the relatively modest level of urban development within the study area and the comparatively mild groundwater pollution, the concentration standards of Class III water were adopted as the reference for Qj concentration representing the external water quality (groundwater).

2.5. Statistical Analysis

For the purpose of statistical analysis and data processing, various software tools were employed, including Excel (Office 365), SPSS 24, Matlab 2016b, and Origin 2019b. These analytical techniques facilitated the rigorous examination and interpretation of the gathered data, allowing for meaningful conclusions to be drawn from the study's findings.

3. Results and Discussion

3.1. Characteristics of Overall Sewage Quality

To minimize the potential error stemming from individual samples, the data collected from three separate samples were averaged and subsequently compared (Figure 2). Notably, a discernible trend of decreasing water quality concentration was observed at H7 from 8 a.m. to 10 p.m., a trend not as pronounced in the other manholes. Additionally, a minor peak was observed at 6 p.m. It is worth noting that during the morning rush hour, the sewage primarily consisted of black water originating from toilets, while the evening rush hour saw a composition mainly comprising detergent and food residue. Specifically, at 8 a.m., the water concentration at H7 significantly exceeded that of the other manholes ($p < 0.001$). From a water quality standpoint, the substantial disparity between H7 and H29 could potentially be attributed to pollutant settling and groundwater dilution. Conversely, no statistically significant differences were observed in terms of organic and nitrogen concentrations between H29 and H38 ($p > 0.05$). The introduction of minor amounts of scattered, unstable sewage between H29 and H38 might potentially attenuate the dilution impact of groundwater.

In a broader context, it is evident that water quality within the same manhole undergoes substantial changes throughout the course of a single day. These fluctuations are closely tied to the shifting water consumption habits of residents in the urban sewage network. To overcome these issues, mixing multiple samples taken at different times within a day has been used in the literature [6]. It is important to underscore that when delving into the study of groundwater infiltration within sewage networks, an extensive dataset of monitoring information is crucial to discerning any underlying patterns or trends. The complexity of factors at play necessitates a robust amount of data to effectively characterize the infiltration patterns and draw meaningful conclusions.

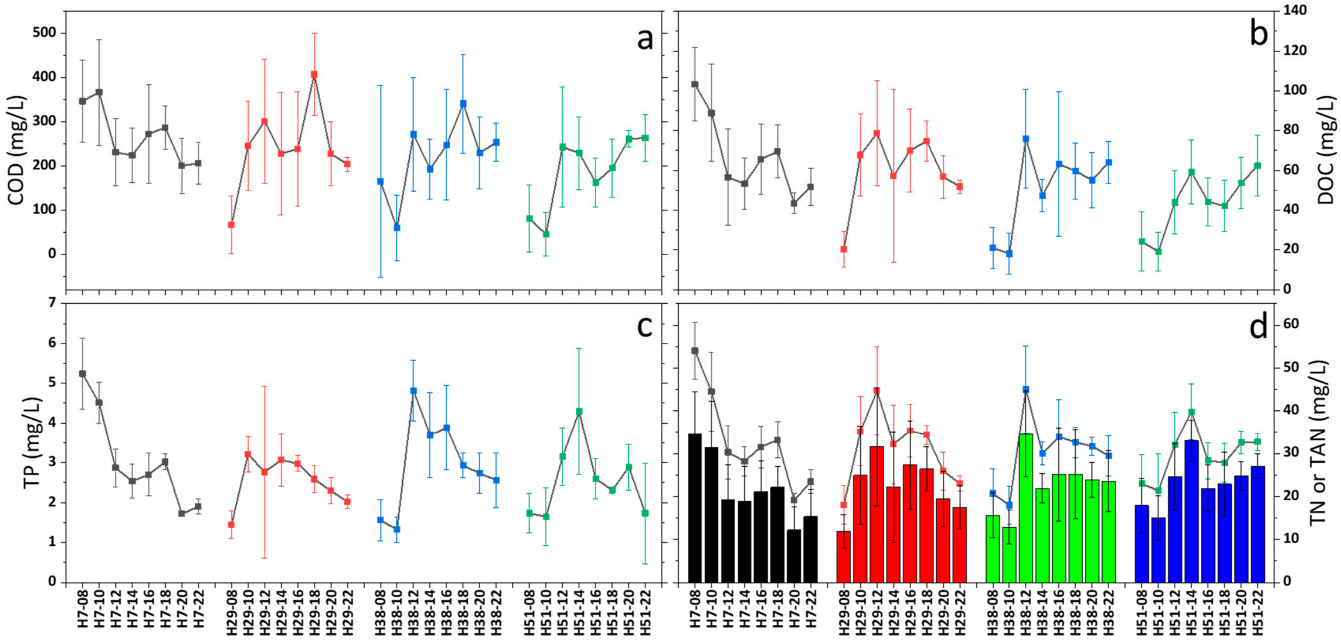

Figure 2. Water quality of each manhole over time: (**a**) COD; (**b**) DOC; (**c**) TP; (**d**) TN and TAN concentrations.

3.2. DOM Fluorescence Characteristics

A total of 64 samples were collected from four manholes during two sampling periods in April and subjected to EEM-parallel factor analysis. Four fluorescent components were extracted and cross-referenced with the OpenFluor database (www.openflour.org, accessed on 20 July 2023) for validation, resulting in the identification of three compounds within the 95% confidence interval. Component A was identified as tryptophan analogs (protein analogs), predominantly originating from domestic wastewater sources [22]. Component B corresponded to humic acid analogs, indicative of microbial activity [23]. Component C was linked to terrestrial humus analogs, primarily sourced from terrestrial soil and freshwater processes, often indicating groundwater influence [24]. The intensity of these fluorescence components across different time intervals for each manhole is graphically presented in Figure 3.

The fluorescence intensity of component A (tryptophan compounds) ranged from 0.0 to 817.9 R.U., with an average of 359.1 ± 192.4 R.U. The fluorescence intensity of component B (humic acid compounds) ranged from 0.0 to 696.7 R.U., with an average of 82.1 ± 147.5 R.U. Component C (terrestrial humus compounds) exhibited fluorescence intensity between 14.5 and 115.2 R.U., with an average of 47.9 ± 17.1 R.U. The total fluorescence intensity spanned from 16.7 to 1136.8 R.U., averaging 481.6 ± 234.3 R.U. The variability in the fluorescence intensity of components A and B can be attributed to temporal variations in domestic sewage discharge. Influenced by the specific mix of production and daily activities of residents during the sampling periods, fluctuations in components A and B, which reflect domestic sewage and microbial activities, were observed. In contrast, the fluorescence intensity of component C remained relatively stable. This stability can be attributed to the consistent migration of external water (groundwater) during sunny days characterized by stable weather conditions and minimal external influences [25,26]. On such days, the extent of groundwater infiltration within the urban sewage network is primarily determined by the network's structural attributes, resulting in relatively minor changes throughout the day.

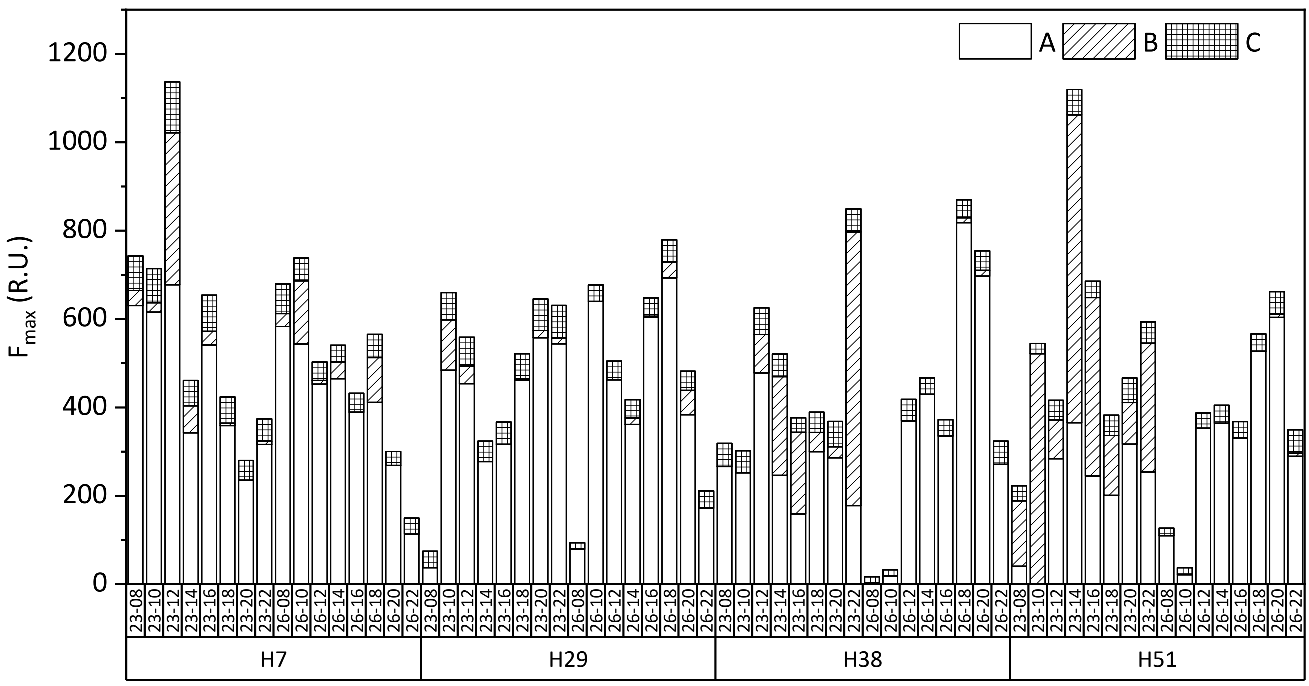

Figure 3. Intensity of fluorescent components at each manhole during the days (23 and 26 April).

From manhole H7 to H29, there was a notable general decrease in the fluorescence intensity of component A. This reduction indicates the additional mixing of low-concentration external water during the transportation process. The proximity between manholes H29 and H38 results in a relatively short transport distance, and direct domestic sewage discharge occurs between these points. The interplay of domestic sewage and groundwater led to no significant distinction in the change in component A between H29 and H38 ($p < 0.05$). In certain time intervals, there was a noteworthy increase in component B for H7 and H38 ($p < 0.001$), possibly influenced by the specific type of domestic sewage discharge during those periods. The significant discrepancy in component B between the two samples from H51 ($p < 0.001$) may be attributed to superior microbial activity and enhanced biodegradability of the domestic sewage introduced from the branch pipe on that particular day. The BOD_5 and COD concentrations for H38 and H51 manholes were recorded as 0.56 ± 0.20 and 0.56 ± 0.22, respectively.

Component C's fluorescence intensity was divided by the sum of the three components, yielding a ratio used to estimate the groundwater proportion (%) (as illustrated in Figure 4). The calculated groundwater proportions for H7, H29, H38, and H51 manholes were $11.7 \pm 4.2\%$, $13.2 \pm 10.3\%$, $18.5 \pm 23.7\%$, and $11.7 \pm 9.0\%$, respectively. Considering the substantial deviations in certain sample values, the groundwater proportions for these four manholes, after eliminating outliers, were adjusted to $10.8 \pm 2.5\%$, $10.8 \pm 3.6\%$, $10.8 \pm 4.1\%$, and $9.6 \pm 3.5\%$. The dispersion observed in the results after excluding outliers remained within a reasonable range, demonstrating that the groundwater proportions adhere to the allowable limits for groundwater infiltration within municipal sewage networks (10–15%) [27]. In developed megacities in China, such as Shenzhen and Shanghai, the groundwater infiltration ratio was reported to be typically more than 25% [28]. The selected sewer network is newly built and is far from any surface water bodies, which might have resulted in the low infiltration ratio. With the increase in service time, a higher infiltration ratio is highly expected [29].

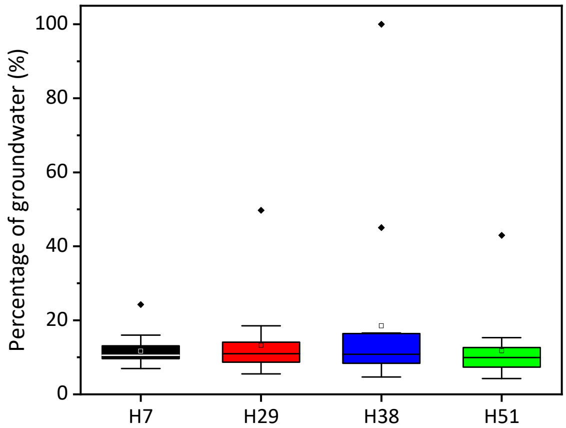

Figure 4. The box plots showing the percentage of groundwater in each inspection well. The box ranges from the first (Q1) to the third quartile (Q3) of the distribution and represents the interquartile range (IQR), with whiskers extending to ±1.5 × IQR; Each outlier outside the whiskers is represented by an individual mark.

3.3. CDOM Source Analysis

Figure 5 presents a comparison of CDOM fluorescence parameters for each manhole. The humification index (HIX) values for organic matter in all manholes remained below 1.5, indicating that the majority of CDOM originated from biological or microbial sources. A small subset of samples from H29, H38, and H51 exhibited HIX values exceeding 1.5 but falling below 2.5. This suggests a weaker humic characteristic and a vital autogenetic trait in CDOM humification, aligning with the distribution reaction of fluorescence intensity for component B. The fluorescence index (FI) values for the samples from each manhole primarily clustered within the range of 1.4–1.9. Specifically, the FI fluorescence indices for H7, H29, H38, and H51 were recorded as 1.75 ± 0.26, 1.55 ± 0.24, 1.65 ± 0.34, and 1.64 ± 0.30, respectively. These values reveal that the H29 segment contained the highest content of both water and land-derived DOM, with the H7 to H29 region being notably impacted by shallow groundwater and the soil layer.

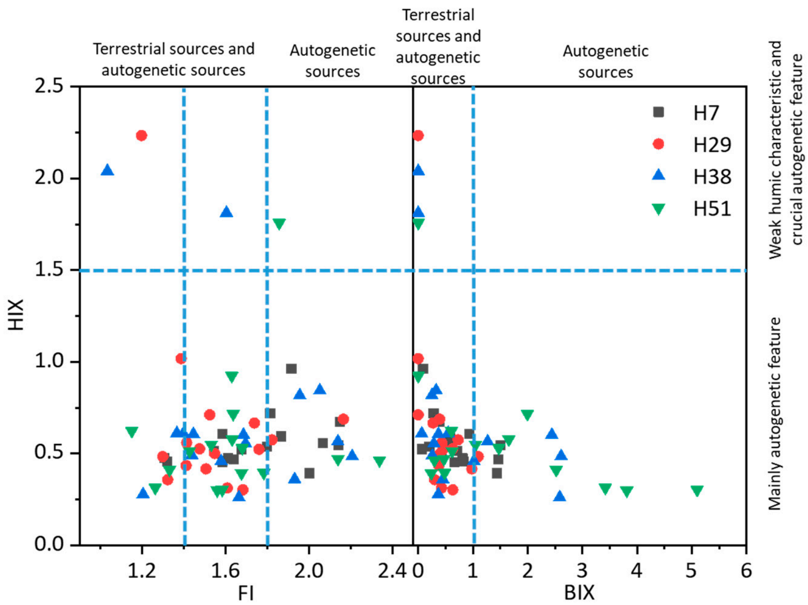

Figure 5. The distribution of CDOM fluorescence parameters for samples from each inspection well. The solid line in the center divides the figure into two panels, i.e., HIX vs. FI on the left, and HIX vs. BIX on the right. The dotted lines represent the threshold for assigning DOM into different sources as stated beside the top and right axes.

The biological index (BIX) values for the four manholes were determined as 0.69 ± 0.47, 0.38 ± 0.44, 0.68 ± 1.10, and 1.40 ± 1.62. Considerable fluctuations in BIX were observed for H38 and H51, which is attributable to the influence of inflow from branch pipes and the combination with groundwater. For the majority of samples, BIX values remained below 1.0, signifying that DOM primarily originated from endogenous and terrestrial sources. These findings align with the results of other indicators examined within this study.

3.4. Calculation of Groundwater Infiltration Based on Water Quality Characterization Factors

By employing total phosphorus (TP) and ammonia nitrogen (TAN) as water quality characteristic factors, the infiltration of groundwater into the sewer system was computed and assessed, as demonstrated in Figure 6. The outcomes for the stretch from H7 to H28 yielded values of 3.54 ± 45.55% (TP) and −16.00 ± 45.36% (TAN), respectively. Conversely, the results for the span from H32 to H51 were 6.94 ± 34.73% (TP) and −8.12 ± 28.04% (TAN), respectively.

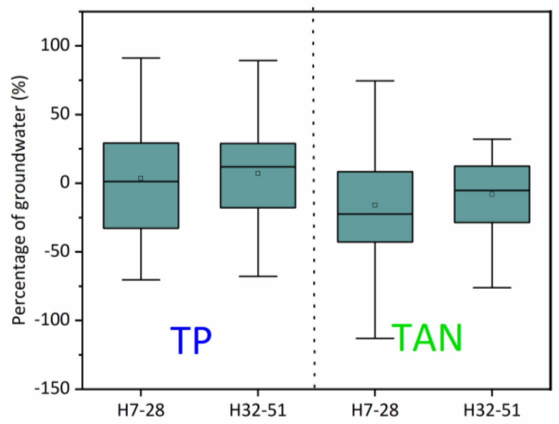

Figure 6. Evaluation of groundwater occupancy in two sewer segments using total phosphorus and ammonia nitrogen as water quality characterization factors. The dotted line separates the plots for total phosphorus (TP) and total ammonia nitrogen (TAN).

It is important to note that the efficacy of groundwater infiltration evaluation using the water quality characteristic factor method is contingent upon precise flow monitoring. Furthermore, deviations in calculation results can arise due to fluctuations in groundwater concentration and the discharge of low-concentration domestic wastewater. In summary, relying on water quality characteristic factors to gauge water infiltration outside the pipeline network may not yield reliable outcomes.

3.5. Principal Component Analysis of Water Quality Parameters

Principal component analysis (PCA) was conducted on each water quality parameter and fluorescence component at every sampling point, and the outcomes are depicted in Figure 7. Intriguingly, the confidence ovals for the four manholes, ranging from upstream to downstream, progressively expand. This observation signifies that the compositional variability within the sewage pipe network escalates downstream, resulting in greater complexity and uncertainty in the composition.

A noteworthy observation is the substantial positive correlation between component B and the autogenic index BIX ($p < 0.001$), affirming the significant relationship between component B and microbial activity. Conversely, component A, component C, chemical oxygen demand (COD), total organic carbon (TOC), biochemical oxygen demand (BOD), total ammonia nitrogen (TAN), and total phosphorus (TP) exhibit positive correlations among themselves. This highlights that employing COD, TOC, BOD, TAN, and TP as water quality characteristic factors for external water infiltration evaluation may not yield dependable outcomes.

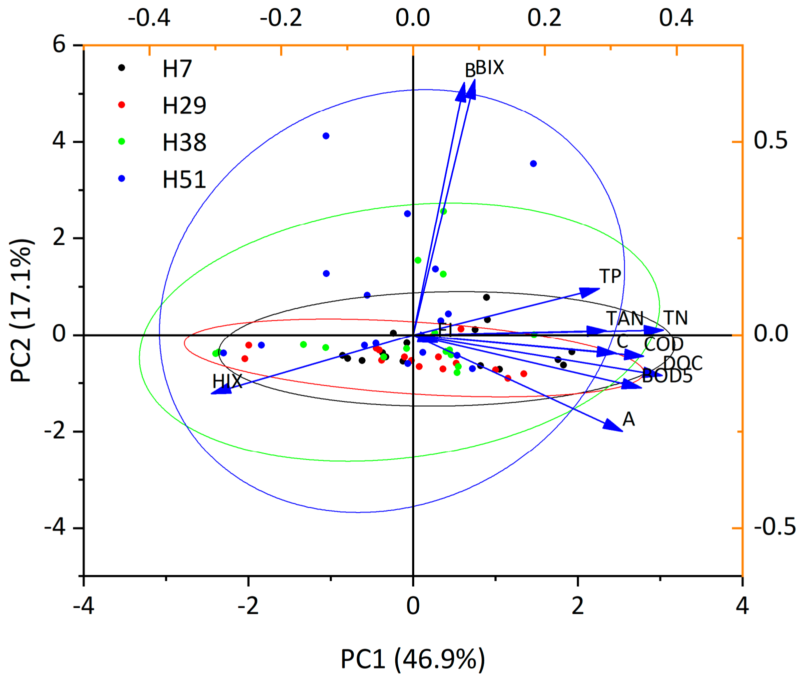

Figure 7. Principal component analysis of water quality parameters for each inspection well. The ellipse indicates the 95% confidence interval of samples from each inspection well; black, H7; red, H29; green, H38; and blue, H51.

4. Conclusions

In the investigation of water quality dynamics and groundwater infiltration within urban sewage networks, relying on data from a single time point is insufficient to accurately depict the network's true condition. To address this limitation, this study undertook continuous water quality monitoring across multiple periods within an eastern Guangdong sewage pipeline network. Employing various methods enhances the reliability of sewage network structural assessment.

Assessing the degree of external water infiltration in urban sewage networks via water quality characteristic factors necessitates precise flow and concentration monitoring. However, this approach is substantially influenced by fluctuations in sewage and external water concentrations, rendering it unreliable due to the extensive data and calculations required. Conversely, employing 3D fluorescence parallel factor analysis enabled the extraction of tryptophan compounds representing domestic sewage, humic acid compounds originating from microbial activities, and terrestrial humus compounds signifying underground water sources. The estimation indicates that the groundwater proportion across the four surveyed inspection wells along the pipeline network ranged from 10.8 $\pm$ 2.5% to 9.6 $\pm$ 3.5%, conforming to the allowable groundwater infiltration limits set for municipal sewage pipelines (10–15%).

The utilization of 3D fluorescence spectrum–parallel factor analysis effectively segregates components originating from distinct dissolved organic matter (CDOM) sources. Consequently, this method serves as a superior benchmark for evaluating external water infiltration. Employing three-dimensional fluorescence spectra enables a more feasible evaluation of external water infiltration, independent of discharge and concentration parameters from diverse pollution sources.

Author Contributions: Conceptualization, L.L., Y.L. and Y.X.; methodology, Y.L. and Y.X.; investigation, L.L., B.F. and H.X.; data curation, P.S., B.F., L.M., Y.G., Z.B. and J.W.; validation, Y.G. and Z.B.; formal analysis, Y.L.; resources, L.M.; writing—original draft preparation, L.L. and Y.L.; writing—review and editing, Y.X.; visualization, J.W.; project administration, P.S.; funding acquisition, H.X. and Y.X. All authors have read and agreed to the published version of the manuscript.

Funding: This research was funded by the Department of Education of Guangdong Province (grant number: 2021ZDZX4016) and the Science and Technology Planning Project of Guangdong Province, China (grant number: 210717176900659).

Data Availability Statement: Not applicable.

Conflicts of Interest: The authors declare no conflict of interest.

References

1. Leal, L.H.; Temmink, H.; Zeeman, G.; Cees, C.J. Comparison of Three Systems for Biological Greywater Treatment. *Water* **2010**, *2*, 155–169. [CrossRef]
2. Wang, C.; Feng, B.; Wang, P.; Guo, W.; Li, X.; Gao, H.; Zhang, B.; Chen, J. Revealing Factors Influencing Spatial Variation in the Quantity and Quality of Rural Domestic Sewage Discharge across China. *Process Saf. Environ. Prot.* **2022**, *162*, 200–210. [CrossRef]
3. Wang, Y.; Lu, X.; Cheng, F. Investigation and Analysis on Rural Domestic Sewage Discharge in Key Watersheds. *IOP Conf. Ser. Earth Environ. Sci.* **2020**, *526*, 012036. [CrossRef]
4. Chen, G.-H.; Leung, D.H.-W.; Huang, J.-C. Removal of Dissolved Organic Carbon in Sanitary Gravity Sewer. *J. Environ. Eng.* **2001**, *127*, 295–301. [CrossRef]
5. Raunkjaer, K.; Hvitved-Jacobsen, T.; Nielsen, P.H. Transformation of Organic Matter in a Gravity Sewer. *Water Environ. Res.* **1995**, *67*, 181–188. [CrossRef]
6. Yang, F.; Zhang, X.; Li, J.; Jin, F.; Zhou, B. Simple Method to Quantify Extraneous Water and Organic Matter Degradation in Sewer Networks. *Environ. Sci. Water Res. Technol.* **2021**, *7*, 172–183. [CrossRef]
7. Qu, J.; Dai, X.; Hu, H.Y.; Huang, X.; Chen, Z.; Li, T.; Cao, Y.; Daigger, G.T. Emerging Trends and Prospects for Municipal Wastewater Management in China. *ACS EST Eng.* **2022**, *2*, 323–336. [CrossRef]
8. Gaona, À.; Solís, B.; Guerrero, J.; Guisasola, A.; Baeza, J.A. Nitrite Pathway in A2/O WWTPs: Modelling Organic Matter Reduction, Operational Cost and N2O Emissions. *J. Clean. Prod.* **2023**, *414*, 137453. [CrossRef]
9. Bagherzadeh, F.; Nouri, A.S.; Mehrani, M.J.; Thennadil, S. Prediction of Energy Consumption and Evaluation of Affecting Factors in a Full-Scale WWTP Using a Machine Learning Approach. *Process Saf. Environ. Prot.* **2021**, *154*, 458–466. [CrossRef]
10. Lee, D.G.; Roehrdanz, P.R.; Feraud, M.; Ervin, J.; Anumol, T.; Jia, A.; Park, M.; Tamez, C.; Morelius, E.W.; Gardea-Torresdey, J.L.; et al. Wastewater Compounds in Urban Shallow Groundwater Wells Correspond to Exfiltration Probabilities of Nearby Sewers. *Water Res.* **2015**, *85*, 467–475. [CrossRef]
11. Wirahadikusumah, R.; Abraham, D.M.; Iseley, T.; Prasanth, R.K. Assessment Technologies for Sewer System Rehabilitation. *Autom. Constr.* **1998**, *7*, 259–270. [CrossRef]
12. Fang, X.; Li, Q.; Zhu, J.; Chen, Z.; Zhang, D.; Wu, K.; Ding, K.; Li, Q. Sewer Defect Instance Segmentation, Localization, and 3D Reconstruction for Sewer Floating Capsule Robots. *Autom. Constr.* **2022**, *142*, 104494. [CrossRef]
13. Haurum, J.B.; Moeslund, T.B. A Survey on Image-Based Automation of CCTV and SSET Sewer Inspections. *Autom. Constr.* **2020**, *111*, 103061. [CrossRef]
14. Sun, L.; Zhu, J.; Tan, J.; Li, X.; Li, R.; Deng, H.; Zhang, X.; Liu, B.; Zhu, X. Deep Learning-Assisted Automated Sewage Pipe Defect Detection for Urban Water Environment Management. *Sci. Total Environ.* **2023**, *882*, 163562. [CrossRef] [PubMed]
15. Mehmood, C.T.; Tan, W.; Chen, Y.; Waheed, H.; Li, Y.; Xiao, Y.; Zhong, Z. UV/O3 Assisted Ceramic Membrane Reactor for Efficient Fouling Control and DOM Transformations in Real Textile Wastewater. *Sep. Purif. Technol.* **2022**, *295*, 121284. [CrossRef]
16. Ifon, B.E.; Adyari, B.; Hou, L.; Ohore, O.E.; Rashid, A.; Yu, C.P.; Anyi, H. Urbanization Influenced the Interactions between Dissolved Organic Matter and Bacterial Communities in Rivers. *J. Environ. Manag.* **2023**, *341*, 117986. [CrossRef]
17. Cohen, E.; Levy, G.J.; Borisover, M. Fluorescent Components of Organic Matter in Wastewater: Efficacy and Selectivity of the Water Treatment. *Water Res.* **2014**, *55*, 323–334. [CrossRef]
18. Stedmon, C.A.; Bro, R. Characterizing Dissolved Organic Matter Fluorescence with Parallel Factor Analysis: A Tutorial. *Limnol. Oceanogr. Methods* **2008**, *6*, 572–579. [CrossRef]
19. Wang, K.; Pang, Y.; He, C.; Li, P.; Xiao, S.; Sun, Y.; Pan, Q.; Zhang, Y.; Shi, Q.; He, D. Optical and Molecular Signatures of Dissolved Organic Matter in Xiangxi Bay and Mainstream of Three Gorges Reservoir, China: Spatial Variations and Environmental Implications. *Sci. Total Environ.* **2019**, *657*, 1274–1284. [CrossRef]
20. Ohno, T. Fluorescence Inner-Filtering Correction for Determining the Humification Index of Dissolved Organic Matter. *Environ. Sci. Technol.* **2002**, *36*, 742–746. [CrossRef]
21. Xu, Y.; Lu, X.; Chen, F. Field Investigation on Rural Domestic Sewage Discharge in a Typical Village of the Taihu Lake Basin. *IOP Conf. Ser. Earth Environ. Sci.* **2020**, *546*, 032031. [CrossRef]
22. Lee, D.; Kwon, M.; Ahn, Y.; Jung, Y.; Nam, S.N.; Choi, I.H.; Kang, J.W. Characteristics of Intracellular Algogenic Organic Matter and Its Reactivity with Hydroxyl Radicals. *Water Res.* **2018**, *144*, 13–25. [CrossRef] [PubMed]
23. Santana-Casiano, J.M.; González-Santana, D.; Devresse, Q.; Hepach, H.; Santana-González, C.; Quack, B.; Engel, A.; González-Dávila, M. Exploring the Effects of Organic Matter Characteristics on Fe(II) Oxidation Kinetics in Coastal Seawater. *Environ. Sci. Technol.* **2022**, *56*, 2718–2728. [CrossRef]

24. Chen, M.; Kim, S.H.; Jung, H.J.; Hyun, J.H.; Choi, J.H.; Lee, H.J.; Huh, I.A.; Hur, J. Dynamics of Dissolved Organic Matter in Riverine Sediments Affected by Weir Impoundments: Production, Benthic Flux, and Environmental Implications. *Water Res.* **2017**, *121*, 150–161. [CrossRef]
25. Li, L.; Huang, M. Analysis of Water Quality Deterioration Based on Groundwater Dynamic Monitoring Results in Maoming Region in 2020. *West. Resour.* **2022**, *6*, 57–62. [CrossRef]
26. Li, B. Study on Nitrogen and Phosphorus Transport Mechanism and Influencing Factors of Lake-Groundwater Driven by Pumping—Taking Longhu Water Source as an Example. Master's Thesis, Chengdu University Techonology, Chengdu, China, 2018.
27. Hu, X.; Lu, M.; Cui, N.; Zhao, P.; Liu, Z.; Liu, X.; Li, H. Hierarchical Diagnostic Technology for Quality and Efficiency Improvement of Urban Drainage Network. *China Water Wastewater* **2023**, *39*, 17–22.
28. Huang, D.; Liu, X.; Jiang, S.; Wang, H.; Wang, J.; Zhang, Y. Current State and Future Perspectives of Sewer Networks in Urban China. *Front. Environ. Sci. Eng.* **2018**, *12*, 2. [CrossRef]
29. Karpf, C.; Krebs, P. Quantification of Groundwater Infiltration and Surface Water Inflows in Urban Sewer Networks Based on a Multiple Model Approach. *Water Res.* **2011**, *45*, 3129–3136. [CrossRef]